Physics Letters B 734 (2014) 122–130

Contents lists available at ScienceDirect

Physics Letters B

www.elsevier.com/locate/physletb

Precision measurement of the ratio of the Λ_b^0 to $\overline{B}^0$ lifetimes

LHCb Collaboration

ARTICLE INFO

Article history:
Received 25 February 2014
Received in revised form 11 April 2014
Accepted 12 May 2014
Available online 16 May 2014
Editor: W.-D. Schlatter

ABSTRACT

The LHCb measurement of the lifetime ratio of the Λ_b^0 baryon to the $\overline{B}^0$ meson is updated using data corresponding to an integrated luminosity of 3.0 fb^{-1} collected using 7 and 8 TeV centre-of-mass energy pp collisions at the LHC. The decay modes used are $\Lambda_b^0 \to J/\psi p K^-$ and $\overline{B}^0 \to J/\psi \pi^+ K^-$, where the $\pi^+ K^-$ mass is consistent with that of the $\overline{K}^{*0}(892)$ meson. The lifetime ratio is determined with unprecedented precision to be $0.974 \pm 0.006 \pm 0.004$, where the first uncertainty is statistical and the second systematic. This result is in agreement with original theoretical predictions based on the heavy quark expansion. Using the current world average of the $\overline{B}^0$ lifetime, the Λ_b^0 lifetime is found to be $1.479 \pm 0.009 \pm 0.010$ ps.

1. Introduction

The heavy quark expansion (HQE) is a powerful theoretical technique in the description of decays of hadrons containing heavy quarks. This model describes inclusive decays and has been used extensively in the analysis of beauty and charm hadron decays, for example in the extraction of Cabibbo–Kobayashi–Maskawa matrix elements, such as $|V_{cb}|$ and $|V_{ub}|$ [1]. The basics of the theory were derived in the late 1980s [2]. For b-flavored hadrons, the expansion of the total decay width in terms of powers of $1/m_b$, where m_b is the b quark mass, was derived a few years later [3]. These developments are summarized in Ref. [4]. It was found that there were no terms of $\mathcal{O}(1/m_b)$, that the $\mathcal{O}(1/m_b^2)$ terms were tiny, and initial estimates of $\mathcal{O}(1/m_b^3)$ [5,6] effects were small. Thus differences of only a few percent were expected between the Λ_b^0 and $\overline{B}^0$ total decay widths, and hence their lifetimes [5,7,8].

In the early part of the past decade, measurements of the ratio of Λ_b^0 to $\overline{B}^0$ lifetimes, $\tau_{\Lambda_b^0}/\tau_{\overline{B}^0}$, gave results considerably smaller than this expectation. In 2003 one experimental average gave 0.798 ± 0.052 [9], while another was 0.786 ± 0.034 [10]. Some authors sought to explain the small value of the ratio by including additional operators or other modifications [11], while others thought that the HQE could be pushed to provide a ratio of about 0.9 [12], but not so low as the measured value. Recent measurements have obtained higher values [13]. In fact, the most precise previous measurement from LHCb, $0.976 \pm 0.012 \pm 0.006$ [14], based on 1.0 fb^{-1} of data, agreed with the early HQE expectations.

In this paper we present an updated result for $\tau_{\Lambda_b^0}/\tau_{\overline{B}^0}$ using data from 3.0 fb^{-1} of integrated luminosity collected with the LHCb detector from pp collisions at the LHC. Here we add the 2.0 fb^{-1} data sample from the 8 TeV data to our previous 1.0 fb^{-1} 7 TeV sample [14]. The data are combined and analyzed together. Larger simulation samples are used than in our previous publication, and uncertainties are significantly reduced.

The Λ_b^0 baryon is detected in the $J/\psi p K^-$ decay mode, discovered by LHCb [14], while the $\overline{B}^0$ meson is reconstructed in $J/\psi \overline{K}^{*0}(892)$ decays, with $\overline{K}^{*0}(892) \to \pi^+ K^-$.[1] These modes have the same topology into four charged tracks, thus facilitating cancellation of systematic uncertainties in the lifetime ratio.

The LHCb detector [15] is a single-arm forward spectrometer covering the pseudorapidity range $2 < \eta < 5$, designed for the study of particles containing b or c quarks. The detector includes a high-precision tracking system consisting of a silicon-strip vertex detector surrounding the pp interaction region, a large-area silicon-strip detector located upstream of a dipole magnet with a bending power of about 4 Tm, and three stations of silicon-strip detectors and straw drift tubes [16] placed downstream. The combined tracking system provides a momentum measurement with relative uncertainty that varies from 0.4% at 5 GeV to 0.6% at 100 GeV, and impact parameter resolution of 20 μm for tracks with large transverse momentum, p_T.[2] Different types of charged hadrons are distinguished using information from two ring-imaging Cherenkov (RICH) detectors [17]. Photon, electron and hadron candidates are identified by a calorimeter system consisting of scintillating-pad and preshower detectors, an electromagnetic calorimeter and a hadronic calorimeter. Muons are

[1] Charge-conjugate modes are implicitly included throughout this Letter.
[2] We use natural units with $\hbar = c = 1$.

http://dx.doi.org/10.1016/j.physletb.2014.05.021

identified by a system composed of alternating layers of iron and multiwire proportional chambers [18]. The trigger [19] consists of a hardware stage, based on information from the calorimeter and muon systems, followed by a software stage, which applies a full event reconstruction.

2. Event selection and b hadron reconstruction

Events selected for this analysis are triggered by a $J/\psi \to \mu^+\mu^-$ decay, where the J/ψ is required at the software level to be consistent with coming from the decay of a b hadron by use of either impact parameter (IP) requirements or detachment of the reconstructed J/ψ decay position from the associated primary vertex.

Events are required to pass a cut-based preselection and then are further filtered using a multivariate discriminator based on the boosted decision tree (BDT) technique [20]. To satisfy the preselection requirements the muon candidates must have $p_{\rm T}$ larger than 550 MeV, while the hadron candidates are required to have $p_{\rm T}$ larger than 250 MeV. Each muon is required to have $\chi^2_{\rm IP} > 4$, where $\chi^2_{\rm IP}$ is defined as the difference in χ^2 of the primary vertex reconstructed with and without the considered track. Events must have a $\mu^+\mu^-$ pair that forms a common vertex with $\chi^2 < 16$ and that has an invariant mass between -48 and $+43$ MeV of the known J/ψ mass [1]. Candidate $\mu^+\mu^-$ pairs are then constrained to the J/ψ mass to improve the determination of the J/ψ momentum. The two charged final state hadrons must have a vector summed $p_{\rm T}$ of more than 1 GeV, and form a vertex with $\chi^2/{\rm ndf} < 10$, where ndf is the number of degrees of freedom, and a common vertex with the J/ψ candidate with $\chi^2/{\rm ndf} < 16$. Particle identification requirements are different for the two modes. Using information from the RICH detectors, a likelihood is formed for each hadron hypothesis. The difference in the logarithms of the likelihoods, ${\rm DLL}(h_1 - h_2)$, is used to distinguish between the two hypotheses, h_1 and h_2 [17]. In the Λ_b^0 decay the kaon candidate must have ${\rm DLL}(K-\pi) > 4$ and ${\rm DLL}(K-p) > -3$, while the proton candidate must have ${\rm DLL}(p-\pi) > 10$ and ${\rm DLL}(p-K) > -3$. For the $\overline{B}^0$ decay, the requirements on the pion candidate are ${\rm DLL}(\pi-\mu) > -10$ and ${\rm DLL}(\pi-K) > -10$, while ${\rm DLL}(K-\pi) > 0$ is required for the kaon.

The BDT selection uses the smaller value of the ${\rm DLL}(\mu-\pi)$ of the μ^+ and μ^- candidates, the $p_{\rm T}$ of each of the two charged hadrons, and their sum, the Λ_b^0 $p_{\rm T}$, the Λ_b^0 vertex χ^2, and the $\chi^2_{\rm IP}$ of the Λ_b^0 candidate with respect to the primary vertex. The choice of these variables is motivated by minimizing the dependence of the selection efficiency on decay time; for example, we do not use the $\chi^2_{\rm IP}$ of the proton, the kaon, the flight distance, or the pointing angle of Λ_b^0 to the primary vertex. To train and test the BDT we use a simulated sample of $\Lambda_b^0 \to J/\psi p K^-$ events for signal and a background data sample from the mass sidebands in the region 100–200 MeV below the Λ_b^0 signal peak. Half of these events are used for training, while the other half are used for testing. The BDT selection is chosen to maximize $S^2/(S+B)$, where S and B are the signal and background yields, respectively. This optimization includes the requirement that the Λ_b^0 candidate decay time be greater than 0.4 ps. The same BDT selection is used for $\overline{B}^0 \to J/\psi\pi^-K^+$ decays. The distributions of the BDT classifier output for signal and background are shown in Fig. 1. The final selection requires that the BDT output variable be greater than 0.04.

The resulting Λ_b^0 and $\overline{B}^0$ candidate invariant mass distributions are shown in Fig. 2. For $\overline{B}^0$ candidates we also require that the invariant π^+K^- mass be within ± 100 MeV of the $\overline{K}^{*0}(892)$ mass. In order to measure the number of signal events we need to ascertain the backgrounds. The background is dominated by random

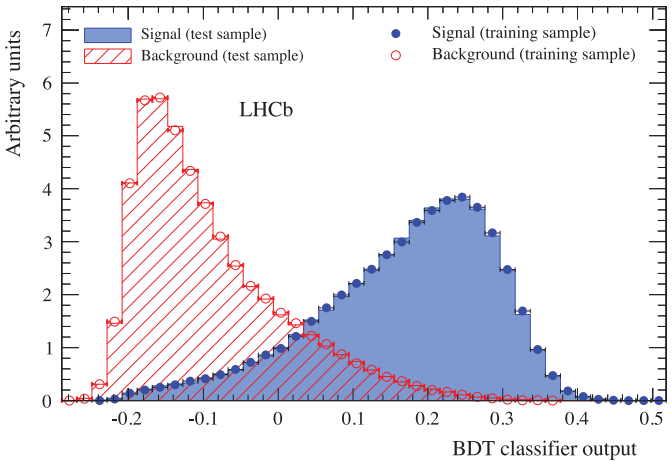

Fig. 1. BDT classifier output for the signal and background. Both training and test samples are shown; their definitions are given in the text.

track combinations at masses around the signal peaks, and their shape is assumed to be exponential in invariant mass. Specific backgrounds arising from incorrect particle identification, called "reflections", are also considered. In the case of the Λ_b^0 decay, these are $\overline{B}_s^0 \to J/\psi K^+K^-$ decays where a kaon is misidentified as a proton and $\overline{B}^0 \to J/\psi \overline{K}^{*0}(892)$ decays with $\overline{K}^{*0}(892) \to \pi^+K^-$ where the pion is misidentified as a proton. There is also a double misidentification background caused by swapping the kaon and proton identifications.

To study these backgrounds, we examine the mass combinations in the sideband regions from 60–200 MeV on either side of the Λ_b^0 mass peak. Specifically for each candidate in the $J/\psi p K^-$ sideband regions we reassign to the proton track the kaon or pion mass hypothesis respectively, and plot them separately. The resulting distributions are shown in Fig. 3. The $m(J/\psi K^+K^-)$ invariant mass distribution shows a large peak at the $\overline{B}_s^0$ mass. There is also a small contribution from the $\overline{B}^0$ final state where the π^+ is misidentified as a p. The $m(J/\psi\pi^+K^-)$ distribution, on the other hand, shows a peak at the $\overline{B}^0$ mass with a large contribution from $\overline{B}_s^0$ decays where the K^+ is misidentified as a p. For both distributions the shapes of the different contributions are determined using simulation. Fitting both distributions we find $19\,327 \pm 309$ $\overline{B}_s^0$, and 5613 ± 285 $\overline{B}^0$ events in the Λ_b^0 sideband.

Samples of simulated $\overline{B}_s^0 \to J/\psi K^+K^-$ and $\overline{B}^0 \to J/\psi K^-\pi^+$ events are used to find the shapes of these reflected backgrounds in the $J/\psi p K^-$ mass spectrum. Using the event yields found in data and the simulation shapes, we estimate 5603 ± 90 $\overline{B}_s^0 \to J/\psi K^+K^-$ and 1150 ± 59 $\overline{B}^0 \to J/\psi\pi^+K^-$ reflection candidates within ± 20 MeV of the Λ_b^0 peak. These numbers are used as Gaussian constraints in the mass fit described below with the central values as the Gaussian means and the uncertainties as the widths. Following a similar procedure we find 1138 ± 48 doubly-misidentified Λ_b^0 decays under the Λ_b^0 peak. This number is also used as a Gaussian constraint in the mass fit.

To determine the number of Λ_b^0 signal candidates we perform an unbinned maximum likelihood fit to the candidate $J/\psi p K^-$ invariant mass spectrum shown in Fig. 2(a). The fit function is the sum of the Λ_b^0 signal component, combinatorial background, the contributions from the $\overline{B}_s^0 \to J/\psi K^+K^-$ and $\overline{B}^0 \to J/\psi\pi^+K^-$ reflections and the doubly-misidentified $\overline{\Lambda_b^0} \to J/\psi K^+\overline{p}$ decays. The signal is modeled by a triple-Gaussian function with common means. The fraction and the width ratio for the second and third Gaussians are fixed to the values obtained in the fit to $\overline{B}^0 \to J/\psi \overline{K}^{*0}(892)$ decays, shown in Fig. 2(b). The effective r.m.s.

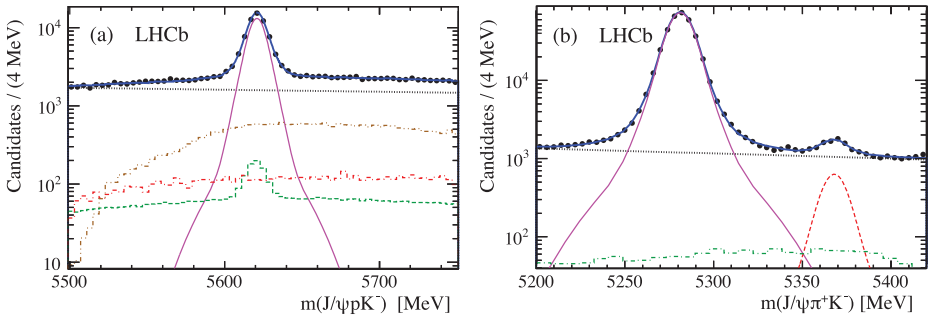

Fig. 2. Fits to the invariant mass spectrum of (a) $J/\psi pK^-$ and (b) $J/\psi\pi^+K^-$ combinations. The Λ_b^0 and $\overline{B}^0$ signals are shown by the (magenta) solid curves. The (black) dotted lines are the combinatorial backgrounds, and the (blue) solid curves show the totals. In (a) the $\overline{B}_s^0 \to J/\psi K^+K^-$ and $\overline{B}^0 \to J/\psi\pi^+K^-$ reflections, caused by particle misidentification, are shown with the (brown) dot-dot-dashed and (red) dot-dashed shapes, respectively, and the (green) dashed shape represents the doubly misidentified $J/\psi K^+\overline{p}$ final state, where the kaon and proton masses are swapped. In (b) the $B_s^0 \to J/\psi\pi^+K^-$ mode is shown by the (red) dashed curve and the (green) dot-dashed shape represents the $\Lambda_b^0 \to J/\psi pK^-$ reflection. (For interpretation of the references to color in this figure legend, the reader is referred to the web version of this article.)

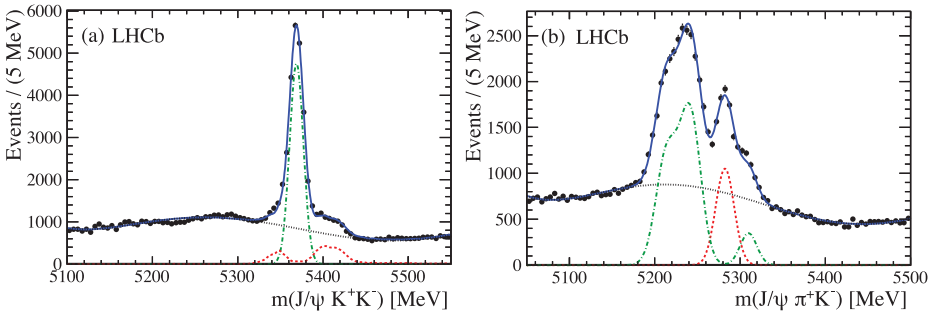

Fig. 3. Invariant mass distributions of $J/\psi pK^-$ data candidates in the sideband regions 60–200 MeV on either side of the Λ_b^0 mass peak, reinterpreted as misidentified (a) $\overline{B}_s^0 \to J/\psi K^+K^-$ and (b) $\overline{B}^0 \to J/\psi\pi^+K^-$ combinations through appropriate mass reassignments. The (red) dashed curves show the $\overline{B}^0$ contributions and the (green) dot-dashed curves show $\overline{B}_s^0$ contributions. The (black) dotted curves represent the polynomial background and the (blue) solid curves the total. (For interpretation of the references to color in this figure legend, the reader is referred to the web version of this article.)

width is 4.7 MeV. The combinatorial background is described by an exponential function. The shapes of reflections and doubly-misidentified contributions are described by histograms imported from the simulations. The mass fit gives $50\,233 \pm 331$ signal and $15\,842 \pm 104$ combinatorial background candidates, 5642 ± 88 $\overline{B}_s^0 \to J/\psi K^+K^-$ and 1167 ± 58 $\overline{B}^0 \to J/\psi\pi^+K^-$ reflection candidates, and 1140 ± 48 doubly-misidentified Λ_b^0 candidates within ± 20 MeV of the Λ_b^0 mass peak. The pK^- mass spectrum is consistent with that found previously [14], with a distinct peak near 1520 MeV, together with the other broad resonant and non-resonant structures that cover the entire kinematic region.

The $\overline{B}^0$ candidate mass distribution can be polluted by the reflection from $\Lambda_b^0 \to J/\psi pK^-$ and $\overline{B}_s^0 \to J/\psi K^+K^-$ decays. Following a similar procedure as for the analysis of the Λ_b^0 mass spectra, we take into account the reflection under the $\overline{B}^0$ peak. Fig. 2(b) shows the fit to the $J/\psi\pi^+K^-$ mass distribution. There are signal peaks at both $\overline{B}^0$ and $\overline{B}_s^0$ masses on top of the background. A triple-Gaussian function with common means is used to fit each signal. The shape of the $B_s^0 \to J/\psi\pi^+K^-$ mass distribution is taken to be the same as that of the signal $\overline{B}^0$ decay. The effective r.m.s. width is 6.5 MeV. An exponential function is used to fit the combinatorial background. The shape of the $\Lambda_b^0 \to J/\psi pK^-$ reflection is taken from simulation, the yield being Gaussian constrained in the global fit to the expected value. The mass fit gives $340\,256 \pm 893$ signal and $11\,978 \pm 153$ background candidates along with a negligible 573 ± 27 contribution of $\Lambda_b^0 \to J/\psi pK^-$ reflection candidates within ± 20 MeV of the $\overline{B}^0$ mass peak. All other reflection contributions are found to be negligible.

3. Measurement of the Λ_b^0 to $\overline{B}^0$ lifetime ratio

The decay time, t, is calculated as

$$t = m\frac{\vec{d}\cdot\vec{p}}{|\vec{p}|^2}, \tag{1}$$

where m is the reconstructed invariant mass, $\vec{p}$ the momentum and $\vec{d}$ the flight distance vector of the particle between the production and decay vertices. The b hadron is constrained to come from the primary vertex. To avoid systematic biases due to shifts in the measured decay time, we do not constrain the two muons to the J/ψ mass.

The decay time distribution of the $\Lambda_b^0 \to J/\psi pK^-$ signal can be described by an exponential function convolved with a resolution function, $G(t-t', \sigma_{\Lambda_b^0})$, where t' is the true decay time, multiplied by an acceptance function, $A_{\Lambda_b^0}(t)$:

$$F_{\Lambda_b^0}(t) = A_{\Lambda_b^0}(t) \times \left[e^{-t'/\tau_{\Lambda_b^0}} \otimes G\left(t-t', \sigma_{\Lambda_b^0}\right)\right]. \tag{2}$$

The ratio of the decay time distributions of $\Lambda_b^0 \to J/\psi pK^-$ and $\overline{B}^0 \to J/\psi \overline{K}^{*0}(892)$ is given by

$$R(t) = \frac{A_{\Lambda_b^0}(t) \times [e^{-t'/\tau_{\Lambda_b^0}} \otimes G(t-t', \sigma_{\Lambda_b^0})]}{A_{\overline{B}^0}(t) \times [e^{-t'/\tau_{\overline{B}^0}} \otimes G(t-t', \sigma_{\overline{B}^0})]}. \tag{3}$$

The advantage of measuring the lifetime through the ratio is that the decay time acceptances introduced by the trigger requirements, selection and reconstruction almost cancel in the ratio of

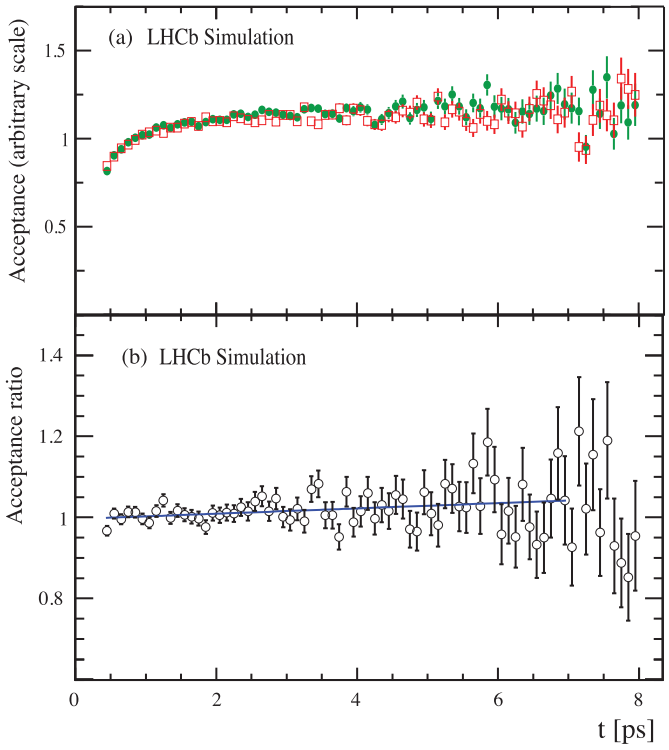

Fig. 4. (a) Decay time acceptances (arbitrary scale) from simulation for (green) circles $\Lambda_b^0 \to J/\psi p K^-$, and (red) open-boxes $\overline{B}^0 \to J/\psi \overline{K}^{*0}(892)$ decays. (b) Ratio of the decay time acceptances between $\Lambda_b^0 \to J/\psi p K^-$ and $\overline{B}^0 \to J/\psi \overline{K}^{*0}(892)$ decays obtained from simulation. The (blue) line shows the result of the linear fit. (For interpretation of the references to color in this figure legend, the reader is referred to the web version of this article.)

the decay time distributions. The decay time resolutions are 40 fs for the Λ_b^0 decay and 37 fs for the $\overline{B}^0$ decay [14]. They are both small enough in absolute scale, and similar enough for differences in resolutions between the two modes not to affect the final result. Thus,

$$R(t) = R(0)e^{-t(1/\tau_{\Lambda_b^0} - 1/\tau_{\overline{B}^0})} = R(0)e^{-t\Delta_{\Lambda B}}, \quad (4)$$

where $\Delta_{\Lambda B} \equiv 1/\tau_{\Lambda_b^0} - 1/\tau_{\overline{B}^0}$ is the width difference and $R(0)$ is the normalization. Since the acceptances are not quite equal, a correction is implemented to first order by modifying Eq. (4) with a linear function

$$R(t) = R(0)[1 + at]e^{-t\Delta_{\Lambda B}}, \quad (5)$$

where a represents the slope of the acceptance ratio as a function of decay time.

The decay time acceptance is the ratio between the reconstructed decay time distribution for selected events and the generated decay time distribution convolved with the triple-Gaussian decay time resolutions obtained from the simulations. In order to ensure that the p and p_T distributions of the generated b hadrons are correct, we weight the simulated samples to match the data distributions. The simulations do not model the hadron identification efficiencies with sufficient accuracy for our purposes. Therefore we further weight the samples according to the hadron identification efficiencies obtained from $D^{*+} \to \pi^+ D^0$, $D^0 \to K^-\pi^+$ events for pions and kaons, and $\Lambda \to p\pi^-$ for protons. The $\Lambda_b^0 \to J/\psi p K^-$ sample is also weighted using signal yields in bins of $m(pK^-)$.

The decay time acceptances obtained from the weighted simulations are shown in Fig. 4(a). The individual acceptances in both cases exhibit the same behaviour. The ratio of the decay time acceptances is shown in Fig. 4(b). For decay times greater than 7 ps, the acceptance is poorly determined, while below 0.4 ps the individual acceptances decrease quickly. Thus, we consider decay times in the range 0.4–7.0 ps. A χ^2 fit to the acceptance ratio with a function of the form $C(1 + at)$ between 0.4 and 7 ps, gives a slope $a = 0.0066 \pm 0.0023$ ps^{-1} and an intercept of $C = 0.996 \pm 0.005$. The χ^2/ndf of the fit is 65/64.

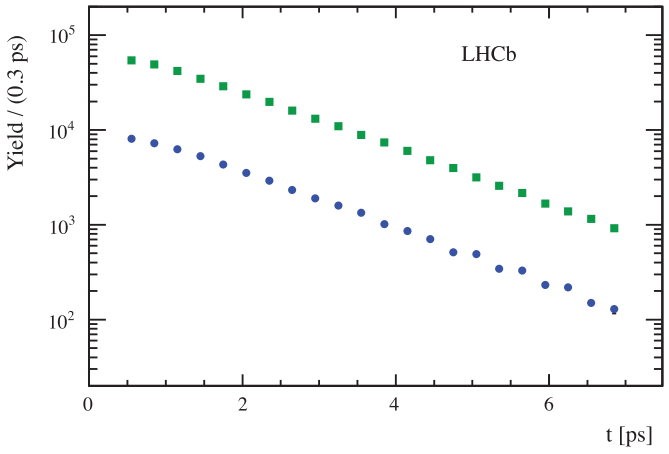

Fig. 5. Decay time distributions for $\Lambda_b^0 \to J/\psi p K^-$ shown as (blue) circles, and $\overline{B}^0 \to J/\psi \overline{K}^{*0}(892)$ shown as (green) squares. For most entries the error bars are smaller than the points. (For interpretation of the references to color in this figure legend, the reader is referred to the web version of this article.)

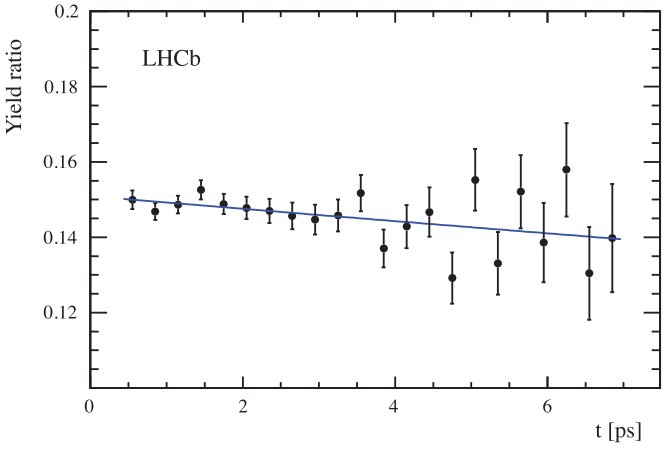

Fig. 6. Decay time ratio between $\Lambda_b^0 \to J/\psi p K^-$ and $\overline{B}^0 \to J/\psi \overline{K}^{*0}(892)$ decays, and the fit for $\Delta_{\Lambda B}$ used to measure the Λ_b^0 lifetime.

In order to determine the ratio of Λ_b^0 to $\overline{B}^0$ lifetimes, we determine the yield of b hadrons for both decay modes using unbinned maximum likelihood fits described in Section 2 to the b hadron mass distributions in 22 bins of decay time of equal width between 0.4 and 7 ps. We use the parameters found from the time integrated fits fixed in each time bin, with the signal and background yields allowed to vary, except for the double misidentification background fraction that is fixed.

The resulting signal yields as a function of decay time are shown in Fig. 5. The subsequent decay time ratio distribution fitted with the function given in Eq. (5) is shown in Fig. 6. A χ^2 fit is used with the slope $a = 0.0066$ ps^{-1} fixed, and both the normalization parameter $R(0)$, and $\Delta_{\Lambda B}$ allowed to vary. The fitted value of the reciprocal lifetime difference is

$$\Delta_{\Lambda B} = 17.9 \pm 4.3 \pm 3.1 \text{ ns}^{-1}.$$

Table 1
Systematic uncertainties on the $\Delta_{\Lambda B}$, the lifetimes ratio $\tau_{\Lambda_b^0}/\tau_{\overline{B}^0}$ and the Λ_b^0 lifetime. The systematic uncertainty associated with $\Delta_{\Lambda B}$ is independent of the $\overline{B}^0$ lifetime.

Source	$\Delta_{\Lambda B}$ (ns^{-1})	$\tau_{\Lambda_b^0}/\tau_{\overline{B}^0}$	$\tau_{\Lambda_b^0}$ (ps)
Signal shape	1.5	0.0021	0.0032
Background model	0.7	0.0010	0.0015
Double misidentification	1.3	0.0019	0.0029
Acceptance slope	2.2	0.0032	0.0049
Acceptance function	0.2	0.0003	0.0004
Decay time fit range	0.3	0.0004	0.0006
pK helicity	0.3	0.0004	0.0006
$\overline{B}^0$ lifetime	–	0.0001	0.0068
Total	3.1	0.0044	0.0096

Whenever two uncertainties are quoted, the first is statistical and second systematic. The latter will be discussed in Section 4. The χ^2/ndf of the fit is 20.3/20. The resulting ratio of lifetimes is

$$\frac{\tau_{\Lambda_b^0}}{\tau_{\overline{B}^0}} = \frac{1}{1+\tau_{\overline{B}^0}\Delta_{\Lambda B}} = 0.974 \pm 0.006 \pm 0.004,$$

where we use the world average value 1.519 ± 0.007 ps for $\tau_{\overline{B}^0}$ [1]. This result is consistent with and more precise than our previously measured value of $0.976 \pm 0.012 \pm 0.006$ [14]. Multiplying the lifetime ratio by $\tau_{\overline{B}^0}$, the Λ_b^0 baryon lifetime is

$$\tau_{\Lambda_b^0} = 1.479 \pm 0.009 \pm 0.010 \text{ ps}.$$

4. Systematic uncertainties

Sources of the systematic uncertainties on $\Delta_{\Lambda B}$, $\tau_{\Lambda_b^0}/\tau_{\overline{B}^0}$ and the Λ_b^0 lifetime are summarized in Table 1. The systematic uncertainty due to the signal model is estimated by comparing the results between the default fit with a triple-Gaussian function and a fit with a double-Gaussian function. We find a change of $\Delta_{\Lambda B} = 1.5$ ns^{-1}, which we assign as the uncertainty. Letting the signal shape parameters free in every time bin results in a change of 0.4 ns^{-1}. The larger of these two variations is taken as the systematic uncertainty on the signal shape.

The uncertainties due to the background are estimated by comparing the default result to that obtained when we allow the exponential background parameter to float in each time bin. We also replace the exponential background function with a linear function; the resulting difference is smaller than the assigned uncertainty due to floating the background shape. The systematic uncertainty due to the normalization of the double misidentification background is evaluated by allowing the fraction to change in each time bin.

The systematic uncertainties due to the acceptance slope are estimated by varying the slope, a, according to its statistical uncertainty from the simulation. An alternative choice of the acceptance function, where a second-order polynomial is used to parametrize the acceptance ratio between $\Lambda_b^0 \to J/\psi p K^-$ and $\overline{B}^0 \to J/\psi \overline{K}^{*0}(892)$, results in a smaller uncertainty. There is also an uncertainty due to the decay time range used because of the possible change of the acceptance ratio at short decay times. This uncertainty is ascertained by changing the fit range to be 0.7–7.0 ps and using the difference with the baseline fit. This uncertainty is greatly reduced with respect to our previous publication [14] due to the larger fit range, finer decay time bins, and larger signal sample.

In order to correctly model the acceptance, which can depend on the kinematics of the decay, the $\Lambda_b^0 \to J/\psi p K^-$ simulation is weighted according to the $m(pK^-)$ distribution observed in data. As a cross-check, we weight the simulation according to the two-dimensional distribution of $m(pK^-)$ and pK^- helicity angle and assign the difference as a systematic uncertainty. In addition, the PDG value for the $\overline{B}^0$ lifetime, $\tau_{\overline{B}^0} = 1.519 \pm 0.007$ ps [1], is used to calculate the Λ_b^0 lifetime; the errors contribute to the systematic uncertainty. The total systematic uncertainty is obtained by adding all of the contributions in quadrature.

5. Conclusions

We determine the ratio of lifetimes of the Λ_b^0 baryon and $\overline{B}^0$ meson to be

$$\frac{\tau_{\Lambda_b^0}}{\tau_{B^0}} = 0.974 \pm 0.006 \pm 0.004.$$

This is the most precise measurement to date and supersedes our previously published result [14]. It demonstrates that the Λ_b^0 lifetime is shorter than the $\overline{B}^0$ lifetime by $-(2.6 \pm 0.7)\%$, consistent with the original predictions of the HQE [2,4,5,21,22], thus providing validation for the theory. Using the world average measured value for the $\overline{B}^0$ lifetime [1], we determine

$$\tau_{\Lambda_b^0} = 1.479 \pm 0.009 \pm 0.010 \text{ ps},$$

which is the most precise measurement to date.

LHCb has also made a measurement of $\tau_{\Lambda_b^0}$ using the $J/\psi\Lambda$ final state obtaining $1.415 \pm 0.027 \pm 0.006$ ps [23]. The two LHCb measurements have systematic uncertainties that are only weakly correlated, and we quote an average of the two measurements of $1.468 \pm 0.009 \pm 0.008$ ps.

Acknowledgements

We are thankful for many useful and interesting conversations with Prof. Nikolai Uraltsev who contributed greatly to theories describing heavy hadron lifetimes; unfortunately he passed away before these results were available. We express our gratitude to our colleagues in the CERN accelerator departments for the excellent performance of the LHC. We thank the technical and administrative staff at the LHCb institutes. We acknowledge support from CERN and from the national agencies: CAPES, CNPq, FAPERJ and FINEP (Brazil); NSFC (China); CNRS/IN2P3 and Region Auvergne (France); BMBF, DFG, HGF and MPG (Germany); SFI (Ireland); INFN (Italy); FOM and NWO (The Netherlands); SCSR (Poland); MEN/IFA (Romania); MinES, Rosatom, RFBR and NRC "Kurchatov Institute" (Russia); MinECo, XuntaGal and GENCAT (Spain); SNSF and SER (Switzerland); NAS Ukraine (Ukraine); STFC (United Kingdom); NSF (USA). We also acknowledge the support received from the ERC under FP7. The Tier1 computing centres are supported by IN2P3 (France), KIT and BMBF (Germany), INFN (Italy), NWO and SURF (The Netherlands), PIC (Spain), GridPP (United Kingdom). We are indebted to the communities behind the multiple open source software packages we depend on. We are also thankful for the computing resources and the access to software R&D tools provided by Yandex LLC (Russia).

References

[1] Particle Data Group, J. Beringer, et al., Review of particle physics, Phys. Rev. D 86 (2012) 010001, and 2013 update for 2014 edition.
[2] M.A. Shifman, M.B. Voloshin, Hierarchy of lifetimes of charmed and beautiful hadrons, Sov. Phys. JETP 64 (1986) 698;
M.A. Shifman, M.B. Voloshin, Preasymptotic effects in inclusive weak decays of charmed particles, Sov. J. Nucl. Phys. 41 (1985) 120;

M.A. Shifman, M.B. Voloshin, On annihilation of mesons built from heavy and light quark and $\bar{B}^0 \leftrightarrow B^0$ oscillations, Sov. J. Nucl. Phys. 45 (1987) 292;
B. Guberina, R. Rückl, J. Trampetić, Charmed baryon lifetime differences, Z. Phys. C 33 (1986) 297.
[3] B. Blok, M.A. Shifman, The rule of discarding $1/N_c$ in inclusive weak decays (I), Nucl. Phys. B 399 (1993) 441, arXiv:hep-ph/9207236;
B. Blok, M.A. Shifman, The rule of discarding $1/N_c$ in inclusive weak decays (II), Nucl. Phys. B 399 (1993) 459, arXiv:hep-ph/9209289;
I.I. Bigi, N.G. Uraltsev, Gluonic enhancements in non-spectator beauty decays: an inclusive mirage though an exclusive possibility, Phys. Lett. B 280 (1992) 271;
I.I. Bigi, N.G. Uraltsev, A.I. Vainshtein, Nonperturbative corrections to inclusive beauty and charm decays: QCD versus phenomenological models, Phys. Lett. B 293 (1992) 430, arXiv:hep-ph/9207214.
[4] I.I. Bigi, et al., Nonleptonic decays of beauty hadrons: from phenomenology to theory, in: S. Stone (Ed.), *B* Decays, revised 2nd edition, World Scientific, Singapore, 1994, pp. 132–157, arXiv:hep-ph/9401298.
[5] M. Neubert, C.T. Sachrajda, Spectator effects in inclusive decays of beauty hadrons, Nucl. Phys. B 483 (1997) 339, arXiv:hep-ph/9603202.
[6] N.G. Uraltsev, On the problem of boosting nonleptonic *b* baryon decays, Phys. Lett. B 376 (1996) 303, arXiv:hep-ph/9602324;
UKQCD Collaboration, M. Di Pierro, C.T. Sachrajda, C. Michael, An exploratory lattice study of spectator effects in inclusive decays of the Λ_b^0 baryon, Phys. Lett. B 468 (1999) 143, arXiv:hep-lat/9906031.
[7] H.-Y. Cheng, Phenomenological analysis of heavy hadron lifetimes, Phys. Rev. D 56 (1997) 2783, arXiv:hep-ph/9704260.
[8] J.L. Rosner, Enhancement of the Λ_b^0 decay rate, Phys. Lett. B 379 (1996) 267, arXiv:hep-ph/9602265.
[9] M. Battaglia, et al., The CKM matrix and the unitarity triangle, in: Proceedings of the Workshop, CERN, Geneva, Switzerland, 13–16 Feb, 2002, arXiv:hep-ph/0304132.
[10] C. Tarantino, Beauty hadron lifetimes and B meson CP violation parameters from lattice QCD, Eur. Phys. J. C 33 (2004) S895, arXiv:hep-ph/0310241;
E. Franco, V. Lubicz, F. Mescia, C. Tarantino, Lifetime ratios of beauty hadrons at the next-to-leading order in QCD, Nucl. Phys. B 633 (2002) 212, arXiv:hep-ph/0203089.
[11] T. Ito, M. Matsuda, Y. Matsui, New possibility of solving the problem of lifetime ratio $\tau_{\Lambda_b^0}/\tau_{\bar{B}^0}$, Prog. Theor. Phys. 99 (1998) 271, arXiv:hep-ph/9705402;
F. Gabbiani, A.I. Onishchenko, A.A. Petrov, Λ_b^0 lifetime puzzle in heavy quark expansion, Phys. Rev. D 68 (2003) 114006, arXiv:hep-ph/0303235;
F. Gabbiani, A.I. Onishchenko, A.A. Petrov, Spectator effects and lifetimes of heavy hadrons, Phys. Rev. D 70 (2004) 094031, arXiv:hep-ph/0407004;
G. Altarelli, G. Martinelli, S. Petrarca, F. Rapuano, Failure of local duality in inclusive nonleptonic heavy flavor decays, Phys. Lett. B 382 (1996) 409, arXiv:hep-ph/9604202.
[12] N.G. Uraltsev, Topics in the heavy quark expansion, arXiv:hep-ph/0010328.
[13] ATLAS Collaboration, G. Aad, et al., Measurement of the Λ_b^0 lifetime and mass in the ATLAS experiment, Phys. Rev. D 87 (2013) 032002, arXiv:1207.2284;
CMS Collaboration, S. Chatrchyan, et al., Measurement of the Λ_b^0 lifetime in pp collisions at $\sqrt{s} = 7$ TeV, J. High Energy Phys. 07 (2013) 163, arXiv:1304.7495;
CDF Collaboration, T. Aaltonen, et al., Measurement of *b* hadron lifetimes in exclusive decays containing a J/ψ in $p\bar{p}$ collisions at $\sqrt{s} = 1.96$ TeV, Phys. Rev. Lett. 106 (2011) 121804, arXiv:1012.3138.
[14] LHCb Collaboration, R. Aaij, et al., Precision measurement of the Λ_b^0 baryon lifetime, Phys. Rev. Lett. 111 (2013) 102003, arXiv:1307.2476.
[15] LHCb Collaboration, A.A. Alves Jr., et al., The LHCb detector at the LHC, J. Instrum. 3 (2008) S08005.
[16] R. Arink, et al., Performance of the LHCb outer tracker, J. Instrum. 9 (2014) 01002, arXiv:1311.3893.
[17] M. Adinolfi, et al., Performance of the LHCb RICH detector at the LHC, Eur. Phys. J. C 73 (2013) 2431, arXiv:1211.6759.
[18] A.A. Alves Jr., et al., Performance of the LHCb muon system, J. Instrum. 8 (2013) P02022, arXiv:1211.1346.
[19] R. Aaij, et al., The LHCb trigger and its performance in 2011, J. Instrum. 8 (2013) P04022, arXiv:1211.3055.
[20] L. Breiman, J.H. Friedman, R.A. Olshen, C.J. Stone, Classification and regression trees, in: Wadsworth International Group, Belmont, California, USA, 1984;
R.E. Schapire, Y. Freund, A decision-theoretic generalization of on-line learning and an application to boosting, J. Comput. Syst. Sci. 55 (1997) 119.
[21] N. Uraltsev, Heavy quark expansion in beauty and its decays, arXiv:hep-ph/9804275.
[22] I.I. Bigi, The QCD perspective on lifetimes of heavy flavor hadrons, arXiv:hep-ph/9508408.
[23] LHCb Collaboration, R. Aaij, et al., Measurements of the B^+, B^0, B_s^0 meson and Λ_b^0 baryon lifetimes, arXiv:1402.2554, JHEP, in press, http://dx.doi.org/10.1016/0370-2693(96)00352-8.

LHCb Collaboration

R. Aaij [41], B. Adeva [37], M. Adinolfi [46], A. Affolder [52], Z. Ajaltouni [5], J. Albrecht [9], F. Alessio [38], M. Alexander [51], S. Ali [41], G. Alkhazov [30], P. Alvarez Cartelle [37], A.A. Alves Jr [25], S. Amato [2], S. Amerio [22], Y. Amhis [7], L. Anderlini [17,g], J. Anderson [40], R. Andreassen [57], M. Andreotti [16,f], J.E. Andrews [58], R.B. Appleby [54], O. Aquines Gutierrez [10], F. Archilli [38], A. Artamonov [35], M. Artuso [59], E. Aslanides [6], G. Auriemma [25,m], M. Baalouch [5], S. Bachmann [11], J.J. Back [48], A. Badalov [36], V. Balagura [31], W. Baldini [16], R.J. Barlow [54], C. Barschel [39], S. Barsuk [7], W. Barter [47], V. Batozskaya [28], Th. Bauer [41], A. Bay [39], J. Beddow [51], F. Bedeschi [23], I. Bediaga [1], S. Belogurov [31], K. Belous [35], I. Belyaev [31], E. Ben-Haim [8], G. Bencivenni [18], S. Benson [50], J. Benton [46], A. Berezhnoy [32], R. Bernet [40], M.-O. Bettler [47], M. van Beuzekom [41], A. Bien [11], S. Bifani [45], T. Bird [54], A. Bizzeti [17,i], P.M. Bjørnstad [54], T. Blake [48], F. Blanc [39], J. Blouw [10], S. Blusk [59], V. Bocci [25], A. Bondar [34], N. Bondar [30], W. Bonivento [15,38], S. Borghi [54], A. Borgia [59], M. Borsato [7], T.J.V. Bowcock [52], E. Bowen [40], C. Bozzi [16], T. Brambach [9], J. van den Brand [42], J. Bressieux [39], D. Brett [54], M. Britsch [10], T. Britton [59], N.H. Brook [46], H. Brown [52], A. Bursche [40], G. Busetto [22,q], J. Buytaert [38], S. Cadeddu [15], R. Calabrese [16,f], O. Callot [7], M. Calvi [20,k], M. Calvo Gomez [36,o], A. Camboni [36], P. Campana [18,38], D. Campora Perez [38], F. Caponio [21], A. Carbone [14,d], G. Carboni [24,l], R. Cardinale [19,j], A. Cardini [15], H. Carranza-Mejia [50], L. Carson [50], K. Carvalho Akiba [2], G. Casse [52], L. Cassina [20], L. Castillo Garcia [38], M. Cattaneo [38], Ch. Cauet [9], R. Cenci [58], M. Charles [8], Ph. Charpentier [38], S.-F. Cheung [55], N. Chiapolini [40], M. Chrzaszcz [40,26], K. Ciba [38], X. Cid Vidal [38], G. Ciezarek [53], P.E.L. Clarke [50], M. Clemencic [38], H.V. Cliff [47], J. Closier [38], C. Coca [29], V. Coco [38], J. Cogan [6], E. Cogneras [5], P. Collins [38], A. Comerma-Montells [36], A. Contu [15,38], A. Cook [46], M. Coombes [46], S. Coquereau [8], G. Corti [38], I. Counts [56], B. Couturier [38], G.A. Cowan [50], D.C. Craik [48], M. Cruz Torres [60], S. Cunliffe [53], R. Currie [50], C. D'Ambrosio [38], J. Dalseno [46], P. David [8], P.N.Y. David [41], A. Davis [57], I. De Bonis [4], K. De Bruyn [41], S. De Capua [54], M. De Cian [11], J.M. De Miranda [1], L. De Paula [2], W. De Silva [57], P. De Simone [18], D. Decamp [4], M. Deckenhoff [9], L. Del Buono [8], N. Déléage [4], D. Derkach [55], O. Deschamps [5], F. Dettori [42], A. Di Canto [11], H. Dijkstra [38], S. Donleavy [52], F. Dordei [11], M. Dorigo [39],

P. Dorosz [26,n], A. Dosil Suárez [37], D. Dossett [48], A. Dovbnya [43], F. Dupertuis [39], P. Durante [38], R. Dzhelyadin [35], A. Dziurda [26], A. Dzyuba [30], S. Easo [49], U. Egede [53], V. Egorychev [31], S. Eidelman [34], S. Eisenhardt [50], U. Eitschberger [9], R. Ekelhof [9], L. Eklund [51,38], I. El Rifai [5], Ch. Elsasser [40], S. Esen [11], A. Falabella [16,f], C. Färber [11], C. Farinelli [41], S. Farry [52], D. Ferguson [50], V. Fernandez Albor [37], F. Ferreira Rodrigues [1], M. Ferro-Luzzi [38], S. Filippov [33], M. Fiore [16,f], M. Fiorini [16,f], C. Fitzpatrick [38], M. Fontana [10], F. Fontanelli [19,j], R. Forty [38], O. Francisco [2], M. Frank [38], C. Frei [38], M. Frosini [17,38,g], J. Fu [21], E. Furfaro [24,l], A. Gallas Torreira [37], D. Galli [14,d], S. Gambetta [19,j], M. Gandelman [2], P. Gandini [59], Y. Gao [3], J. Garofoli [59], J. Garra Tico [47], L. Garrido [36], C. Gaspar [38], R. Gauld [55], L. Gavardi [9], E. Gersabeck [11], M. Gersabeck [54], T. Gershon [48], Ph. Ghez [4], A. Gianelle [22], S. Giani' [39], V. Gibson [47], L. Giubega [29], V.V. Gligorov [38], C. Göbel [60], D. Golubkov [31], A. Golutvin [53,31,38], A. Gomes [1,a], H. Gordon [38], M. Grabalosa Gándara [5], R. Graciani Diaz [36], L.A. Granado Cardoso [38], E. Graugés [36], G. Graziani [17], A. Grecu [29], E. Greening [55], S. Gregson [47], P. Griffith [45], L. Grillo [11], O. Grünberg [61], B. Gui [59], E. Gushchin [33], Yu. Guz [35,38], T. Gys [38], C. Hadjivasiliou [59], G. Haefeli [39], C. Haen [38], T.W. Hafkenscheid [64], S.C. Haines [47], S. Hall [53], B. Hamilton [58], T. Hampson [46], S. Hansmann-Menzemer [11], N. Harnew [55], S.T. Harnew [46], J. Harrison [54], T. Hartmann [61], J. He [38], T. Head [38], V. Heijne [41], K. Hennessy [52], P. Henrard [5], L. Henry [8], J.A. Hernando Morata [37], E. van Herwijnen [38], M. Heß [61], A. Hicheur [1], D. Hill [55], M. Hoballah [5], C. Hombach [54], W. Hulsbergen [41], P. Hunt [55], N. Hussain [55], D. Hutchcroft [52], D. Hynds [51], M. Idzik [27], P. Ilten [56], R. Jacobsson [38], A. Jaeger [11], E. Jans [41], P. Jaton [39], A. Jawahery [58], F. Jing [3], M. John [55], D. Johnson [55], C.R. Jones [47], C. Joram [38], B. Jost [38], N. Jurik [59], M. Kaballo [9], S. Kandybei [43], W. Kanso [6], M. Karacson [38], T.M. Karbach [38], M. Kelsey [59], I.R. Kenyon [45], T. Ketel [42], B. Khanji [20], C. Khurewathanakul [39], S. Klaver [54], O. Kochebina [7], I. Komarov [39], R.F. Koopman [42], P. Koppenburg [41], M. Korolev [32], A. Kozlinskiy [41], L. Kravchuk [33], K. Kreplin [11], M. Kreps [48], G. Krocker [11], P. Krokovny [34], F. Kruse [9], M. Kucharczyk [20,26,38,k], V. Kudryavtsev [34], K. Kurek [28], T. Kvaratskheliya [31,38], V.N. La Thi [39], D. Lacarrere [38], G. Lafferty [54], A. Lai [15], D. Lambert [50], R.W. Lambert [42], E. Lanciotti [38], G. Lanfranchi [18], C. Langenbruch [38], B. Langhans [38], T. Latham [48], C. Lazzeroni [45], R. Le Gac [6], J. van Leerdam [41], J.-P. Lees [4], R. Lefèvre [5], A. Leflat [32], J. Lefrançois [7], S. Leo [23], O. Leroy [6], T. Lesiak [26], B. Leverington [11], Y. Li [3], M. Liles [52], R. Lindner [38], C. Linn [38], F. Lionetto [40], B. Liu [15], G. Liu [38], S. Lohn [38], I. Longstaff [51], J.H. Lopes [2], N. Lopez-March [39], P. Lowdon [40], H. Lu [3], D. Lucchesi [22,q], H. Luo [50], E. Luppi [16,f], O. Lupton [55], F. Machefert [7], I.V. Machikhiliyan [31], F. Maciuc [29], O. Maev [30,38], S. Malde [55], G. Manca [15,e], G. Mancinelli [6], M. Manzali [16,f], J. Maratas [5], U. Marconi [14], C. Marin Benito [36], P. Marino [23,s], R. Märki [39], J. Marks [11], G. Martellotti [25], A. Martens [8], A. Martín Sánchez [7], M. Martinelli [41], D. Martinez Santos [42], F. Martinez Vidal [63], D. Martins Tostes [2], A. Massafferri [1], R. Matev [38], Z. Mathe [38], C. Matteuzzi [20], A. Mazurov [16,38,f], M. McCann [53], J. McCarthy [45], A. McNab [54], R. McNulty [12], B. McSkelly [52], B. Meadows [57,55], F. Meier [9], M. Meissner [11], M. Merk [41], D.A. Milanes [8], M.-N. Minard [4], J. Molina Rodriguez [60], S. Monteil [5], D. Moran [54], M. Morandin [22], P. Morawski [26], A. Mordà [6], M.J. Morello [23,s], R. Mountain [59], F. Muheim [50], K. Müller [40], R. Muresan [29], B. Muryn [27], B. Muster [39], P. Naik [46], T. Nakada [39], R. Nandakumar [49], I. Nasteva [1], M. Needham [50], N. Neri [21], S. Neubert [38], N. Neufeld [38], A.D. Nguyen [39], T.D. Nguyen [39], C. Nguyen-Mau [39,p], M. Nicol [7], V. Niess [5], R. Niet [9], N. Nikitin [32], T. Nikodem [11], A. Novoselov [35], A. Oblakowska-Mucha [27], V. Obraztsov [35], S. Oggero [41], S. Ogilvy [51], O. Okhrimenko [44], R. Oldeman [15,e], G. Onderwater [64], M. Orlandea [29], J.M. Otalora Goicochea [2], P. Owen [53], A. Oyanguren [36], B.K. Pal [59], A. Palano [13,c], F. Palombo [21,t], M. Palutan [18], J. Panman [38], A. Papanestis [49,38], M. Pappagallo [51], L. Pappalardo [16], C. Parkes [54], C.J. Parkinson [9], G. Passaleva [17], G.D. Patel [52], M. Patel [53], C. Patrignani [19,j], C. Pavel-Nicorescu [29], A. Pazos Alvarez [37], A. Pearce [54], A. Pellegrino [41], M. Pepe Altarelli [38], S. Perazzini [14,d], E. Perez Trigo [37], P. Perret [5], M. Perrin-Terrin [6], L. Pescatore [45], E. Pesen [65], G. Pessina [20], K. Petridis [53], A. Petrolini [19,j], E. Picatoste Olloqui [36], B. Pietrzyk [4], T. Pilař [48], D. Pinci [25], A. Pistone [19], S. Playfer [50], M. Plo Casasus [37], F. Polci [8], A. Poluektov [48,34], E. Polycarpo [2], A. Popov [35], D. Popov [10], B. Popovici [29], C. Potterat [36], A. Powell [55], J. Prisciandaro [39], A. Pritchard [52], C. Prouve [46], V. Pugatch [44], A. Puig Navarro [39], G. Punzi [23,r], W. Qian [4], B. Rachwal [26], J.H. Rademacker [46], B. Rakotomiaramanana [39], M. Rama [18], M.S. Rangel [2], I. Raniuk [43], N. Rauschmayr [38], G. Raven [42], S. Reichert [54], M.M. Reid [48], A.C. dos Reis [1], S. Ricciardi [49], A. Richards [53], K. Rinnert [52], V. Rives Molina [36], D.A. Roa Romero [5], P. Robbe [7], D.A. Roberts [58], A.B. Rodrigues [1], E. Rodrigues [54], P. Rodriguez Perez [37], S. Roiser [38], V. Romanovsky [35], A. Romero Vidal [37],

M. Rotondo [22], J. Rouvinet [39], T. Ruf [38], F. Ruffini [23], H. Ruiz [36], P. Ruiz Valls [36], G. Sabatino [25,l], J.J. Saborido Silva [37], N. Sagidova [30], P. Sail [51], B. Saitta [15,e], V. Salustino Guimaraes [2], B. Sanmartin Sedes [37], R. Santacesaria [25], C. Santamarina Rios [37], E. Santovetti [24,l], M. Sapunov [6], A. Sarti [18], C. Satriano [25,m], A. Satta [24], M. Savrie [16,f], D. Savrina [31,32], M. Schiller [42], H. Schindler [38], M. Schlupp [9], M. Schmelling [10], B. Schmidt [38], O. Schneider [39], A. Schopper [38], M.-H. Schune [7], R. Schwemmer [38], B. Sciascia [18], A. Sciubba [25], M. Seco [37], A. Semennikov [31], K. Senderowska [27], I. Sepp [53], N. Serra [40], J. Serrano [6], P. Seyfert [11], M. Shapkin [35], I. Shapoval [16,43,f], Y. Shcheglov [30], T. Shears [52], L. Shekhtman [34], O. Shevchenko [43], V. Shevchenko [62], A. Shires [9], R. Silva Coutinho [48], G. Simi [22], M. Sirendi [47], N. Skidmore [46], T. Skwarnicki [59], N.A. Smith [52], E. Smith [55,49], E. Smith [53], J. Smith [47], M. Smith [54], H. Snoek [41], M.D. Sokoloff [57], F.J.P. Soler [51], F. Soomro [39], D. Souza [46], B. Souza De Paula [2], B. Spaan [9], A. Sparkes [50], F. Spinella [23], P. Spradlin [51], F. Stagni [38], S. Stahl [11], O. Steinkamp [40], S. Stevenson [55], S. Stoica [29], S. Stone [59,*], B. Storaci [40], S. Stracka [23,38], M. Straticiuc [29], U. Straumann [40], R. Stroili [22], V.K. Subbiah [38], L. Sun [57], W. Sutcliffe [53], S. Swientek [9], V. Syropoulos [42], M. Szczekowski [28], P. Szczypka [39,38], D. Szilard [2], T. Szumlak [27], S. T'Jampens [4], M. Teklishyn [7], G. Tellarini [16,f], E. Teodorescu [29], F. Teubert [38], C. Thomas [55], E. Thomas [38], J. van Tilburg [11], V. Tisserand [4], M. Tobin [39], S. Tolk [42], L. Tomassetti [16,f], D. Tonelli [38], S. Topp-Joergensen [55], N. Torr [55], E. Tournefier [4,53], S. Tourneur [39], M.T. Tran [39], M. Tresch [40], A. Tsaregorodtsev [6], P. Tsopelas [41], N. Tuning [41], M. Ubeda Garcia [38], A. Ukleja [28], A. Ustyuzhanin [62], U. Uwer [11], V. Vagnoni [14], G. Valenti [14], A. Vallier [7], R. Vazquez Gomez [18], P. Vazquez Regueiro [37], C. Vázquez Sierra [37], S. Vecchi [16], J.J. Velthuis [46], M. Veltri [17,h], G. Veneziano [39], M. Vesterinen [11], B. Viaud [7], D. Vieira [2], X. Vilasis-Cardona [36,o], A. Vollhardt [40], D. Volyanskyy [10], D. Voong [46], A. Vorobyev [30], V. Vorobyev [34], C. Voß [61], H. Voss [10], J.A. de Vries [41], R. Waldi [61], C. Wallace [48], R. Wallace [12], S. Wandernoth [11], J. Wang [59], D.R. Ward [47], N.K. Watson [45], A.D. Webber [54], D. Websdale [53], M. Whitehead [48], J. Wicht [38], J. Wiechczynski [26], D. Wiedner [11], G. Wilkinson [55], M.P. Williams [48,49], M. Williams [56], F.F. Wilson [49], J. Wimberley [58], J. Wishahi [9], W. Wislicki [28], M. Witek [26], G. Wormser [7], S.A. Wotton [47], S. Wright [47], S. Wu [3], K. Wyllie [38], Y. Xie [50,38], Z. Xing [59], Z. Yang [3], X. Yuan [3], O. Yushchenko [35], M. Zangoli [14], M. Zavertyaev [10,b], F. Zhang [3], L. Zhang [59,*], W.C. Zhang [12], Y. Zhang [3], A. Zhelezov [11], A. Zhokhov [31], L. Zhong [3], A. Zvyagin [38]

[1] *Centro Brasileiro de Pesquisas Físicas (CBPF), Rio de Janeiro, Brazil*
[2] *Universidade Federal do Rio de Janeiro (UFRJ), Rio de Janeiro, Brazil*
[3] *Center for High Energy Physics, Tsinghua University, Beijing, China*
[4] *LAPP, Université de Savoie, CNRS/IN2P3, Annecy-Le-Vieux, France*
[5] *Clermont Université, Université Blaise Pascal, CNRS/IN2P3, LPC, Clermont-Ferrand, France*
[6] *CPPM, Aix-Marseille Université, CNRS/IN2P3, Marseille, France*
[7] *LAL, Université Paris-Sud, CNRS/IN2P3, Orsay, France*
[8] *LPNHE, Université Pierre et Marie Curie, Université Paris Diderot, CNRS/IN2P3, Paris, France*
[9] *Fakultät Physik, Technische Universität Dortmund, Dortmund, Germany*
[10] *Max–Planck–Institut für Kernphysik (MPIK), Heidelberg, Germany*
[11] *Physikalisches Institut, Ruprecht–Karls–Universität Heidelberg, Heidelberg, Germany*
[12] *School of Physics, University College Dublin, Dublin, Ireland*
[13] *Sezione INFN di Bari, Bari, Italy*
[14] *Sezione INFN di Bologna, Bologna, Italy*
[15] *Sezione INFN di Cagliari, Cagliari, Italy*
[16] *Sezione INFN di Ferrara, Ferrara, Italy*
[17] *Sezione INFN di Firenze, Firenze, Italy*
[18] *Laboratori Nazionali dell'INFN di Frascati, Frascati, Italy*
[19] *Sezione INFN di Genova, Genova, Italy*
[20] *Sezione INFN di Milano Bicocca, Milano, Italy*
[21] *Sezione INFN di Milano, Milano, Italy*
[22] *Sezione INFN di Padova, Padova, Italy*
[23] *Sezione INFN di Pisa, Pisa, Italy*
[24] *Sezione INFN di Roma Tor Vergata, Roma, Italy*
[25] *Sezione INFN di Roma La Sapienza, Roma, Italy*
[26] *Henryk Niewodniczanski Institute of Nuclear Physics Polish Academy of Sciences, Kraków, Poland*
[27] *AGH – University of Science and Technology, Faculty of Physics and Applied Computer Science, Kraków, Poland*
[28] *National Center for Nuclear Research (NCBJ), Warsaw, Poland*
[29] *Horia Hulubei National Institute of Physics and Nuclear Engineering, Bucharest-Magurele, Romania*
[30] *Petersburg Nuclear Physics Institute (PNPI), Gatchina, Russia*
[31] *Institute of Theoretical and Experimental Physics (ITEP), Moscow, Russia*
[32] *Institute of Nuclear Physics, Moscow State University (SINP MSU), Moscow, Russia*
[33] *Institute for Nuclear Research of the Russian Academy of Sciences (INR RAN), Moscow, Russia*
[34] *Budker Institute of Nuclear Physics (SB RAS) and Novosibirsk State University, Novosibirsk, Russia*
[35] *Institute for High Energy Physics (IHEP), Protvino, Russia*
[36] *Universitat de Barcelona, Barcelona, Spain*
[37] *Universidad de Santiago de Compostela, Santiago de Compostela, Spain*

[38] European Organization for Nuclear Research (CERN), Geneva, Switzerland
[39] Ecole Polytechnique Fédérale de Lausanne (EPFL), Lausanne, Switzerland
[40] Physik-Institut, Universität Zürich, Zürich, Switzerland
[41] Nikhef National Institute for Subatomic Physics, Amsterdam, The Netherlands
[42] Nikhef National Institute for Subatomic Physics and VU University Amsterdam, Amsterdam, The Netherlands
[43] NSC Kharkiv Institute of Physics and Technology (NSC KIPT), Kharkiv, Ukraine
[44] Institute for Nuclear Research of the National Academy of Sciences (KINR), Kyiv, Ukraine
[45] University of Birmingham, Birmingham, United Kingdom
[46] H.H. Wills Physics Laboratory, University of Bristol, Bristol, United Kingdom
[47] Cavendish Laboratory, University of Cambridge, Cambridge, United Kingdom
[48] Department of Physics, University of Warwick, Coventry, United Kingdom
[49] STFC Rutherford Appleton Laboratory, Didcot, United Kingdom
[50] School of Physics and Astronomy, University of Edinburgh, Edinburgh, United Kingdom
[51] School of Physics and Astronomy, University of Glasgow, Glasgow, United Kingdom
[52] Oliver Lodge Laboratory, University of Liverpool, Liverpool, United Kingdom
[53] Imperial College London, London, United Kingdom
[54] School of Physics and Astronomy, University of Manchester, Manchester, United Kingdom
[55] Department of Physics, University of Oxford, Oxford, United Kingdom
[56] Massachusetts Institute of Technology, Cambridge, MA, United States
[57] University of Cincinnati, Cincinnati, OH, United States
[58] University of Maryland, College Park, MD, United States
[59] Syracuse University, Syracuse, NY, United States
[60] Pontifícia Universidade Católica do Rio de Janeiro (PUC-Rio), Rio de Janeiro, Brazil [u]
[61] Institut für Physik, Universität Rostock, Rostock, Germany [v]
[62] National Research Centre Kurchatov Institute, Moscow, Russia [w]
[63] Instituto de Fisica Corpuscular (IFIC), Universitat de Valencia-CSIC, Valencia, Spain [x]
[64] KVI – University of Groningen, Groningen, The Netherlands [y]
[65] Celal Bayar University, Manisa, Turkey [z]

* Corresponding authors.
[a] Universidade Federal do Triângulo Mineiro (UFTM), Uberaba-MG, Brazil.
[b] P.N. Lebedev Physical Institute, Russian Academy of Science (LPI RAS), Moscow, Russia.
[c] Università di Bari, Bari, Italy.
[d] Università di Bologna, Bologna, Italy.
[e] Università di Cagliari, Cagliari, Italy.
[f] Università di Ferrara, Ferrara, Italy.
[g] Università di Firenze, Firenze, Italy.
[h] Università di Urbino, Urbino, Italy.
[i] Università di Modena e Reggio Emilia, Modena, Italy.
[j] Università di Genova, Genova, Italy.
[k] Università di Milano Bicocca, Milano, Italy.
[l] Università di Roma Tor Vergata, Roma, Italy.
[m] Università della Basilicata, Potenza, Italy.
[n] AGH – University of Science and Technology, Faculty of Computer Science, Electronics and Telecommunications, Kraków, Poland.
[o] LIFAELS, La Salle, Universitat Ramon Llull, Barcelona, Spain.
[p] Hanoi University of Science, Hanoi, Viet Nam.
[q] Università di Padova, Padova, Italy.
[r] Università di Pisa, Pisa, Italy.
[s] Scuola Normale Superiore, Pisa, Italy.
[t] Università degli Studi di Milano, Milano, Italy.
[u] Associated to Universidade Federal do Rio de Janeiro (UFRJ), Rio de Janeiro, Brazil.
[v] Associated to Physikalisches Institut, Ruprecht–Karls–Universität Heidelberg, Heidelberg, Germany.
[w] Associated to Institute of Theoretical and Experimental Physics (ITEP), Moscow, Russia.
[x] Associated to Universitat de Barcelona, Barcelona, Spain.
[y] Associated to Nikhef National Institute for Subatomic Physics, Amsterdam, The Netherlands.
[z] Associated to European Organization for Nuclear Research (CERN), Geneva, Switzerland.